Importance of structure and its measurement in quantifying function of forest ecosystems

H. H. Shugart,[1] S. Saatchi,[2] and F. G. Hall[3]

Received 28 February 2009; revised 12 February 2010; accepted 20 May 2010; published 20 November 2010.

[1] The structure of forests, the three-dimensional arrangement of individual trees, has a profound effect on how ecosystems function and cycle carbon, water, and nutrients. The increased need to understand local to global dynamics of ecosystems, a prerequisite to understand the coupling of the biosphere to other components of Earth systems, has created a demand for extensive ecosystem structure data. Repeated satellite observations of vegetation patterns in two dimensions have made significant contributions to our understanding of the state and dynamics of the global biosphere. Recent advances in remote sensing technology allow us to view the biosphere in three dimensions and provide us with refined measurements of horizontal, as well as vertical, structure of forests. This paper provides an introductory review of the importance of the three-dimensional characterization of terrestrial ecosystem structure of forests and woodlands and its potential measurement from space. We discuss the relevance of these measurements for reducing the uncertainties of terrestrial carbon cycle and the response of ecosystems to future climate. By relating the 3-D structure to forest biomass, carbon content, disturbance characteristics, and habitat diversity, we examine the requirements for future satellite sensors in terms of precision and spatial and temporal resolutions. In particular, we focus this review on measurements from lidar and radar sensors that provide vertical and horizontal characterization of vegetation and are currently recommended for next generation of NASA's Earth observing and European Earth Explorer systems.

Citation: Shugart, H. H., S. Saatchi, and F. G. Hall (2010), Importance of structure and its measurement in quantifying function of forest ecosystems, *J. Geophys. Res.*, *115*, G00E13, doi:10.1029/2009JG000993.

1. Introduction

[2] That there is a causal relation between the form of biological systems and their function permeates biology at all scales and has done so over the history of biology as a science. Form influences function; function influences form: the three-dimensional geometry of proteins determines their function as enzymes; the function of being parasitic selects for worms with the strikingly unusual proportions of internal organ sizes; the morphology of a predator's tooth indicates how it feeds, flight constrains the shape of a birds wing; … In this paradigm, form and function are so interactive that knowing both is necessary for understanding.

[3] We consider the influence of form (in this case the "structure" of forests, the physical arrangement of the trees in three dimensions) on the functioning of forests at annual time scales and over larger spatial resolutions. The classic work on this topic is *Watt*'s [1947] paper. Pattern and process is the form-and-function construct at ecological space and time scales. Our discussions here focus on spatial scales from trees, to the gap openings and closures within a forest stand, and then extend to landscape heterogeneities. On the temporal scale, the annual or subannual variations are considered because several important ecosystem processes (energy, water, carbon cycling) emerge at these scales. In this context, we examine how new data obtained from the deployment of active lidar and radar remote sensing satellite systems can improve our understanding of forest structure. Such an improved understanding at a global scale is essential to the planet's biotic diversity and to the functioning of essential global cycles connecting the atmosphere, ocean and biosphere.

1.1. Shape, Size, and Mass of Trees

[4] The structure of a forest can be thought of a consequence of the statistical distribution of the sizes of trees over an area. Typically, tree size is quantified as a diameter (measured at "breast height" of 4.5 feet or 1.3 m and denoted as DBH) and its canopy or stem height (measured at the top of the canopy or below the first branch). The breast-height level is partially a matter of conveniently taking diameter measurements in the field while standing but it also serves to avoid the complexity that most trees swell near the ground as

[1]Department of Environmental Sciences, University of Virginia, Charlottesville, Virginia, USA.
[2]Jet Propulsion Laboratory, California Institute of Technology, Pasadena, California, USA.
[3]NASA Goddard Space Flight Center, Greenbelt, Maryland, USA.

Copyright 2010 by the American Geophysical Union.
0148-0227/10/2009JG000993

the tree trunk transitions into the structural root system. The problem of how to measure tree diameters can be problematic for two of many examples: tropical trees that have deeply fluted or buttressed trunks; trees with multiple trunks. Tree heights are also difficult to measure in the field because of the complexity of measurement techniques and the difficulty of seeing the top of the canopy in dense forests [*West*, 2009].

[5] In general, trees are constrained in their geometry and display striking regularities in their structure. These regularities allow tree diameter to be transformed into other variables of interest. There are two prevalent explanations for these regularities. One involves the mechanical strength required to support standing wood structures; the other, the constraints of transporting water up a tall structure composed of hollow tubes. Trees essentially respond to both of these constraints by developing a complex, but regular architecture that can be characterized, in either case, by the use of statistically calibrated equations known as allometric equations. Tree diameter also can be related to other attributes, such as total tree mass, the area of a tree's foliage, etc. by allometric equations [*McMahon and Bonner*, 1983; *Ter-Mikaelian and Korzukhin*, 1997; *West et al.*, 1999, 1997; *West and Brown*, 2005; *Chave et al.*, 2005]. In general, most trees do not grow symmetrically over their life spans. Small trees have a disproportionally larger amount of leaves and less woody tissue than large trees [*Hallé and Oldemann*, 1975; *Hallé et al.*, 1978].

[6] Structural models based on mechanical strength for wood were initially derived from the engineering problem of building light ship's masts of a given strength [*Greenhill*, 1881; *McMahon*, 1973]. The basic equation for a mast shaped like a tall cone is

$$l = 0.851[E/\rho]^{1/3} d^{2/3}$$

where l is the height of a mast at the point of buckling under its own weight, E is the modulus of elasticity of the wood; ρ is the density of the wood; d is the diameter of the mast at its base.

[7] When these equations are applied to trees one finds that the diameter of record-holding large trees is about a factor of 4 greater than that predicted by their buckling point [*McMahon and Kronauer*, 1976]. Models related to the hydraulic constraints on tree architecture, often referred to as "pipe models," are based on a simple function of the form [*Shinozaki et al.*, 1964; *West et al.*, 1999]

$$d_1 = a d_2^z$$

where d_1 and d_2 are dimensions of the tree (diameter, biomass, leaf area, etc.) and a and z are scalar parameters. There is considerable evidence that the hydraulic constraints on tree structure scale-up to the stand level in the existence of relatively consistent relations between the area of sapwood on a forest stand and the leaf area of the stand [*Waring and Running*, 1997]. These measurements are somewhat confounded by the statistical estimation of sapwood and leaf area as a function of tree diameters on a site. Nonetheless, the relationships hold for many species over different landscapes and are consistent with the underlying assumptions in the pipe model [*Shinozaki et al.*, 1964]. The same hydraulic constraints on tree architecture imply that increased tree height results in less efficient transport of water per unit sapwood area [*McDowell et al.*, 2001]. This theory proposes that the decline of forest productivity with age is a consequence of the loss of hydraulic conductance with increased tree height [*Ryan and Yoder*, 1997]. The limits to tree height have been a subject of numerous studies with the conclusion that trees grow tall only when resources (water, light, nutrients) are abundant [*Niklas and Spatz*, 2004; *Niklas*, 1994; *Koch et al.*, 2004].

[8] In general, one can find an allometric relationship between tree height and sapwood area that scales isometrically, on average, with the tree trunk cross section [*Niklas and Spatz*, 2004]. This relationship varies as a consequence of morphological and ecophysiological species-specific responses to different habitats and hydraulic constraints [*Fulton*, 1999; *Koch et al.*, 2004]. However, it will ultimately converge on an approximately 2/3 scaling rule as the size of the tree increases [*McMahon*, 1973]. Similarly, hydraulic models also imply that there is a scaling relationship between plant diameter and biomass, but they can vary across species due to differences in biomass partitioning patterns and ecological responses to different environmental conditions [*Niklas*, 1994].

[9] The empirical relationship between biomass and tree diameters is difficult to obtain logistically, particularly for remote locations and tropical forests. Most calibrations are sparse with respect to data on larger diameter trees. Since the equations are fitted from log-transformed data, this means that the error bars associated with the larger diameter trees are very large [*Chave et al.*, 2005; *Chambers et al.*, 2001]. In mature natural forests, a large percentage of the total mass is associated with the largest trees, so this is potentially a significant source of error. There are also errors associated with the log transformation of the tree diameters in regression statistics that generate estimation bias [*Beauchamp and Olson*, 1973; *Sprugel*, 1983].

1.2. Structure of Forests

[10] Given a sample of tree diameters and appropriate allometric functions, one can estimate the biomass of a forest as the summation of the biomass of the trees comprising the forest. There are some important scale-related implications in this simple procedure. Averaging the forest biomass reduces the variation seen in the biomass estimates of individual trees. There is evidence that for many forests an aggregation of about 1 ha provides a significant amount of variability reduction [*Weishampel et al.*, 1992, 1994; *Shugart et al.*, 2000; *Hurtt et al.*, 2010]. At smaller spatial scales variability in forest biomass is large, suggesting that there are significant forest features that are seen at one spatial scale and not others [*Chave et al.*, 2003] (Figure 1). While averaging results from small size plots reduces the variance due to error in the tree-biomass-estimation procedure, it also masks biomass variability resulting from spatial structural variability [*Weishampel et al.*, 1992, 1994]. This variability arises from tree-to-tree competitive interactions that often occur at the scale of a large canopy tree.

[11] When only one tree species is present, the competition becomes extremely important when the forest stand reaches a "self-exclusion" or thinning stage. A self-thinning may reduce the number of stems in an area by about 90% in 50 years [*Tadaki et al.*, 1977]. There is an upper limit to the

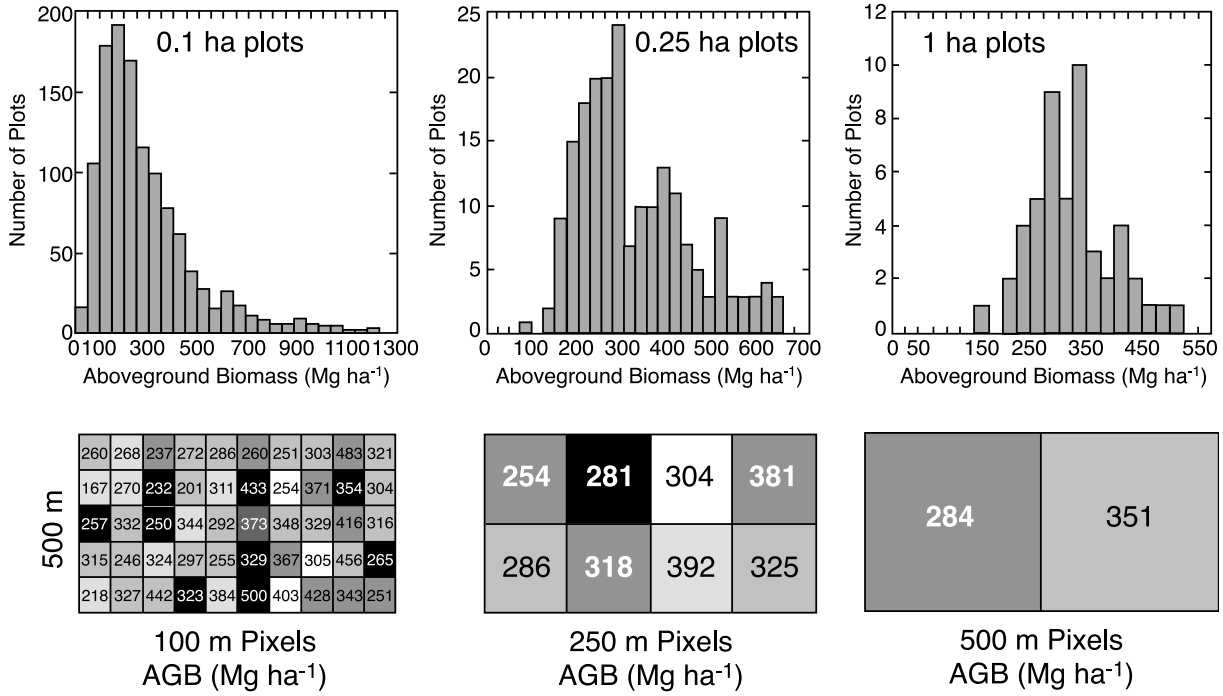

Figure 1. Aboveground biomass distribution in subplots within a 50 ha permanent plot in tropical wet forests of Barro Colorado Island, Panama (R. Condit, 1995; data downloaded from https://ctfs.arnarb.harvard.edu/webatlas/). The distribution is skewed and unsymmetric at 0.1 ha, representing the gap dynamics, and almost symmetric and normal at 1.0 ha, representing forest structure at equilibrium. By increasing the size of subplots to 250 m and 500 m, the values of biomass show less variability.

number of stems within an area as a function of average biomass of individual trees [*White*, 1981]. This relationship is often presented in a log-log plot that has a nearly constant slope of −3/2. There is a decrease in tree numbers with increasing average size of the trees [*Waring and Running*, 1997]. Debris from tree mortality can have a significant influence on soil organic matter by increasing the nutrients and impacting the regeneration [*Landsberg and Waring*, 1997].

[12] To understand the significance of structure on forest biomass, two cases are discussed: (1) the even-aged stands with one species of tree and (2) forest biomass in complex stands with mixed-age structure and multiple species.

1.2.1. Even-Aged, Monospecies Forest Stands

[13] Even-aged forest stands are the product of more than 200 years of forestry practice spread over Europe, particularly Northern Europe, after forests had been substantially cleared over Medieval times [*Williams*, 2003]. From about 1800, forestry practice transitioned from earlier exploitive extraction of material to a more "trees as a crop" agricultural management of forest tracts. Eventually, a forest modeling concept called the "yield table" approach developed and became the signature of modern forestry. Nowadays, some of the historical forest data sets used in yield tables have grown to very long records [*Pretzsch*, 2009]. Piecing together of yield tables from stands on similar sites but of different ages (what ecologists would term "space for time" substitution) has extended some yield table records to 200+ years of predictions.

[14] The organization of yield tables is based on the assumption that on a given kind of site (same soils, same rainfall, etc.) trees in monospecies and even-aged stands grow to the same height at a given age, regardless of density of trees. For trees of the same heights, at low densities one would expect trees with large diameters and crowns; at an equivalent high-density location the trees would have smaller diameters and crowns. In a yield table, forest stand data are arranged by the height of the trees at a given location at a reference age which is usually the typical age of tree harvest. The tree height at this standard age is called a "site index" and is used to signify the overall quality of a location for growing trees. Using yield tables, one can assess the volume of wood in managed stands of equivalent heights on different sites. Two significant observations arise from consideration of yield tables.

[15] 1. One can obtain an empirically based indication of the capability of height measurements to predict forest biomass by multiplying the forest wood volume with the wood density. In Figure 2, the variation of tree volume ranges over 125 m^3 ha^{-1} (or ±12.5% of the average volume of 500 m^3 ha^{-1} over the range of different site index stands when the dominant canopy height is 30 m. This 30 m height would occur at a later age for sites with low site index stands and vice versa.

[16] 2. The rate of mortality of trees in stands undergoing natural thinning is highest in stands with the highest site indices. Faster growing trees suppress their competitors at a higher rate than slower growing trees on low site index locations.

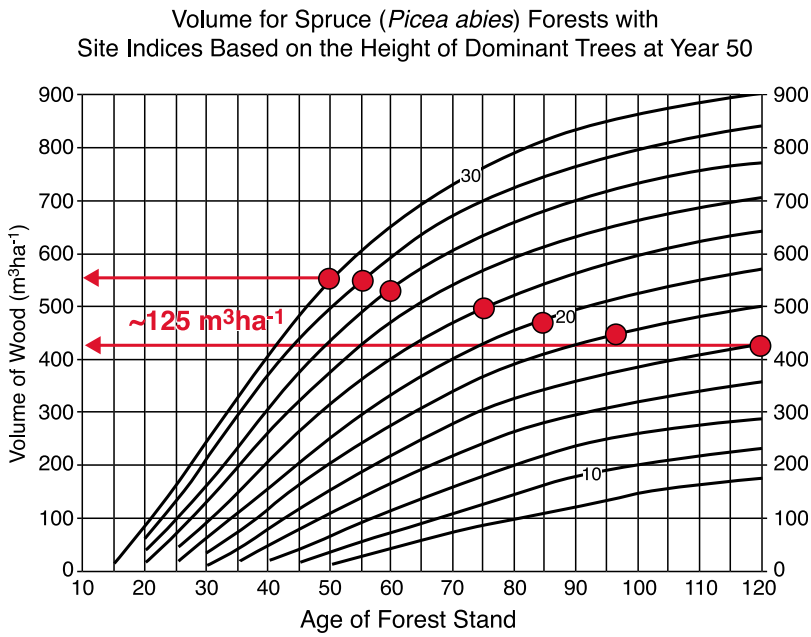

Figure 2. Sections of stand yield tables for Switzerland. Plot of stand age (*x* axis) versus wood volume (*y* axis). The families of curves represent forests with different site indices (an index of site quality that is the expected height of the dominant trees in even-aged stands of spruce (*Picea abies*) at an age of 50 years). Note that this data set covers 120 years of measurement and is based on survey plots covering over 100 years of measurements. Some of these plots were initially developed and regularly resurveyed starting as early as 1888. Other plots have been added and resurveyed over this passage of time [*Köhl et al.*, 1995]. The volume of wood in a forest increases with age and slows in its rate of increase over time. Sites with higher site indices have more wood volume at any given time. The red circles on each of the site index based curves indicate the age when canopy dominant trees in stands of each size class reach a 30 m height. The solid red lines project the age points for stands with the highest and lowest site indices to the associated volume of wood in each stand. The range in wood volumes is about 125 m^3 ha^{-1} or ±12.5%. Modified from Erragstafeln: Fichte. Eidgenössische Anstalt für das forstliche Versuchswesen, Birmensdorf ZH [see *Köhl et al.*, 1995].

[17] The trade-off between rapid tree growth versus high mortality on good sites is the basis of the development of thinning strategies for managed stands and for schemes to plant forest plantations at particular spacing of trees. Despite the elevated mortality, sites with high site indices are more productive than low site index locations.

[18] Single-species, even-aged stands also occur as natural forests. For the vast boreal forest, one finds extensive forest recovering from wildfires that are dominated by single species and of the same age. For most of the northern and midlatitude forests, average height of forest stands is considered an indicator of site quality and growth potential and is usually derived from the forest age height relationship [*Kimmins*, 1987; *Kira*, 2001]. However, height alone does not provide the aboveground biomass of natural forests with the required precision for carbon management. In a recent study of northern and midlatitude forests (Figure 3), it was found that average height can be used as a proxy for large-scale biomass variations and is a critical factor for controlling the magnitude of regional biomass density [*Fang et al.*, 2006]. Data from individual forest plots indicate that average height can explain approximately 60% of biomass variation on the regional scales [*Fang et al.*, 2006] (see Figure 3).

1.2.2. Mixed-Aged, Multispecies Forest Stands

[19] While height is a central feature in forestry yield tables for single species and even-aged forests, the predictive power of height can become weaker in mature or old-growth forests. There, dominant trees often do not show any appreciable height growth and height may even decline in senescing but still dominant canopy trees. However, diameters continue to increase, adding to the biomass of trees. In boreal forests, maximum biomass can approach 400 $Mgha^{-1}$ although average biomass may be only 40 $Mgha^{-1}$ [*Botkin and Simpson*, 1990]. Similarly in temperate and topical forests, the average biomass may be 200 $Mgha^{-1}$ and 330 $Mgha^{-1}$, respectively [*Brown et al.*, 1991], but the maximum biomass may reach 2500 $Mgha^{-1}$ in Pacific Northwest of U.S. or 690 $Mgha^{-1}$ in tropical Asia. The relative contributions of diameter and height in determining the forest biomass have been evaluated with recent allometric equations developed for tropical forests [*Chave et al.*, 2005].

[20] Disturbance and recovery of forest ecosystems are essential to the understanding of the temporal dynamics of the biomass development in mature forests and its role in the global carbon cycle [see *Houghton et al.*, 2009]. *Watt* [1947] developed a classic concept that the structure of a mature forest (at the scale of several hectares) is a heterogeneous mixture of patches in different phases or stages of recovery

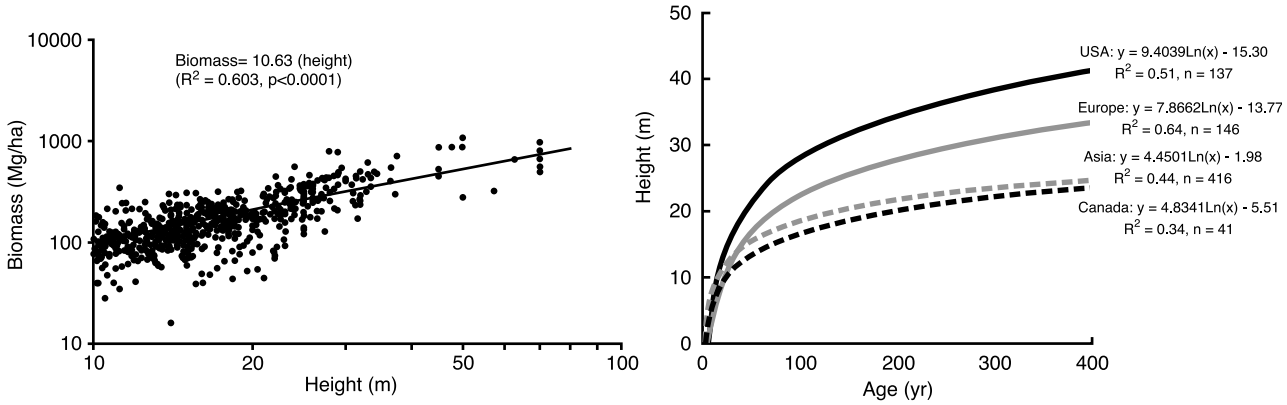

Figure 3. Average forest height predicts the aboveground biomass of even-aged and managed forests of northern midlatitude forests: (left) continental scale relationship of biomass and average height from 645 forest plots with a canopy taller than 10 m to represent closed canopy forests and (right) relationships between mean forest age and forest height for the northern regions (United States, Canada, East Asia, and Europe), suggesting the highest overall site quality is in U.S. forests, followed by European, Asian, and Canadian forests (modified from *Fang et al.* [2006] with kind permission from Springer Science and Business Media).

from disturbance and gap-phase replacement. The mature forest should have patches with all stages of gap-phase dynamics and the areal proportions of each should reflect different gap replacement stages. This has significant implications for the apparent dynamics of forests when viewed at different spatial resolution. The biomass dynamics for a single-canopy-sized piece of a forest (Figure 4a) is quasi-cyclical in the form of a sawtoothed curve [*Shugart*, 1998]. The spaces between the "teeth" in the sawtooth curve are determined by how long a particular tree lives and how much time is required for a new tree to grow to dominate a canopy gap. At a landscape scale, the overall biomass dynamic (Figure 4b) is determined by summing the dynamics of the parts of the mosaic (summation of several sawtooth curves). If there has been a synchronizing event, such as a clear cutting, one would expect the mosaic biomass curve to follow four stages of development: In the first stage of regrowth, the curve rises uniformly because all patches of forests are simultaneously covered with growing trees (I in Figure 4b). At the second stage, the mosaic biomass curve levels out because of continuous growth of dominant trees in some patches are balanced by the loss of biomass due to competition and mortality in other patches (II in Figure 4b). If the trees over the area have relatively similar longevities, there is also a subsequent period when several (perhaps the majority) of the pieces that comprise the forest mosaic all have deaths of the canopy dominant trees (III in Figure 4b). Over time, the local biomass dynamics become desynchronized and the biomass curve varies about some quasi-equilibrium level (IV in Figure 4b).

[21] The occurrence of such patterns has been documented for several different mature forest systems. The presence of shade-intolerant trees in patches of mature undisturbed forest is one observation consistent with the mosaic dynamics of mature forests (for tropical rain forests see *Whitmore* [1982] for review and discussion as well as *Jansen et al.* [2008]; see also *Manabe et al.* [2009] for warm temperate forests and *Kenderes et al.* [2008] for cool temperate forests). The spatial scale of these patterns is important in designing measurement approaches to capture the biomass of the mosaic forest or the dynamics occurring at gap-filling patches. The scales of the mosaics in many natural forests are somewhat larger than one would expect from gap filling of single tree gaps [*Rackham*, 1992] indicating an importance of phenomena that cause multiple tree replacements. Also, the relatively long records (ca. 40 years in most cases) that are available for different forests show the spatial scales where the processes of mortality and recruitment impact the forest composition and biomass development (see *Jones* [1945] and *Rackham* [1992] for temperate forests and see *Swaine and Hall* [1988] for tropical forest examples).

1.2.3. Modeling Forest Dynamics at Different Scales

[22] In general, forests can be studied at two spatial scales that are represented by a set of sampling scales: At a large scale, a forest stand seeks an equilibrium state with a particular mean configuration. This state once attained remains the same, thereafter. At a small scale (the so-called the gap scale), the forest ecosystem never reaches an equilibrium state and is continuously undergoing changes driven by the presence of large trees. For example, at 0.1 ha scale, forest dynamics are nonequilibrium seeking and quasi-cyclical; at hectare scale the dynamics are equilibrium seeking. The demarcation between these two modes of behavior is on the order of the size of the tree canopy of dominant trees (10 m to 30 m implying a 0.01 to 0.1 ha area). It is typically larger in temperate and boreal forests and smaller in tropical rain forest [*Kuuluvainen*, 1992].

[23] Regardless of the ecosystem type, the mechanisms that define the scales are very similar. At the scale of gap dynamics, the forest undergoes a characteristic dynamic that is explained in terms of demographic mechanisms and life history traits of the species involved [*Huston and Smith*, 1987]. At the larger scale of the forest stand, attributes such as stand biomass, diameter distributions, and species composition are variables that express the integration or steady state condition of forest dynamics under a set of environmental conditions [*Smith and Urban*, 1988]. At any

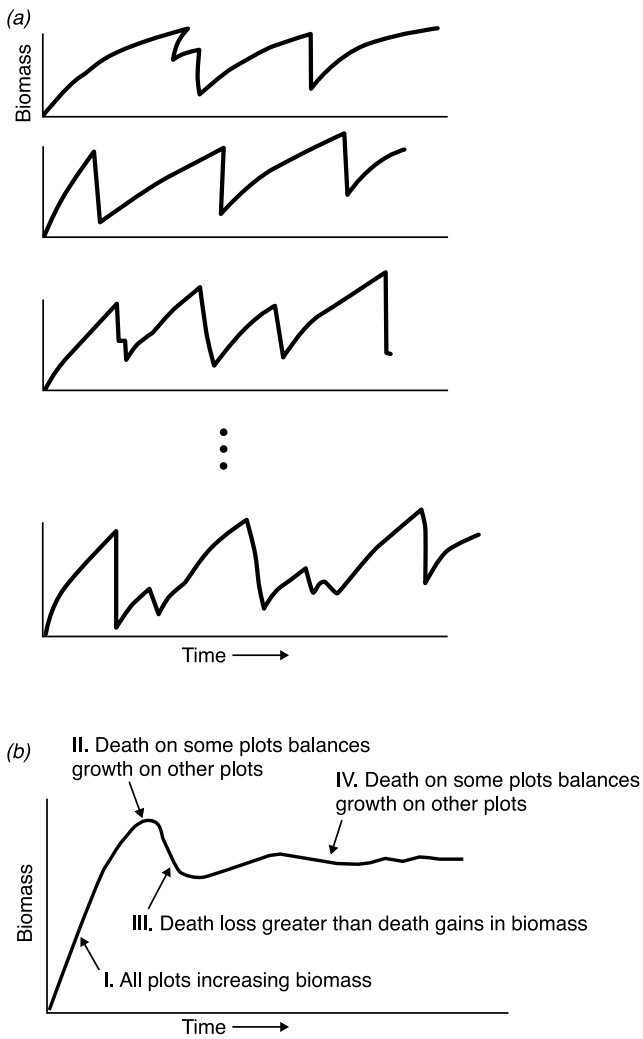

Figure 4. Biomass dynamics for an idealized landscape. The response is from a relatively large, homogeneous area composed of small patches with gap-phase biomass dynamics. (a) The individual dynamics of the patches that are summed to produce (b) the landscape biomass dynamics. The landscape biomass dynamics curve has four sections indicated: I, increasing landscape biomass curve rising as all of the patches are simultaneously covered with growing trees; II, local drops in biomass are balanced by the continued growth of large trees at other locations (the landscape biomass curve levels out); III, if the trees have relatively similar longevities, there is a period when several (perhaps the majority) of the patches that comprise the forest mosaic all have deaths of the canopy dominant trees; IV, the local biomass dynamics become desynchronized and the landscape biomass curve varies about some level.

intermediate states, forest structural configuration or behaviors is not coherent and cannot be interpreted easily. This suggests that the choice of a reference scale and the sampling method are important to capture both qualitative patterns and quantitative characteristics of forest stands.

[24] One of the significant implications of this spatial-scale related difference in the apparent fundamental behavior of a forest is its impact on the resolution and the sampling density of forest structure or biomass. To characterize the landscape-scale biomass variations, plots or remote sensing resolutions of 1.0 ha is more appropriate because it captures the equilibrium state or the aggregate pattern of the forest. However, plot sizes or spatial resolutions of 0.1 ha (or less), are more suitable to sample the nonequilibrium state of the forest and capture the processes controlling the forest dynamics (see Figure 1). The interactions at the finer scales reveal the mechanisms that would drive future dynamic change in forest structure. These 0.1 ha scale dynamics are largely lost in the averaging to coarser-scale forest characterizations. While this finding is from a model-based simulation, it uses a spatially explicit version of a class of models that have been able to reproduce a broad array of forest pattern and dynamics and that have been considered for applications involving responses of forests to global environmental change [*Shugart*, 1990; *Shugart and Prentice*, 1992; *Shugart et al.*, 1992, 1996].

[25] Forests often display distinct layering, with different pools of species associated with each layer. In rain forests (where the structure is the most complex), these include: forest floor, herb layer, shrub layer, understory, canopy, and emergents [*Richards*, 1953; *Baker and Wilson*, 2000]. *Brunig et al.* [1979] found that if one sampled a tropical rain forest using relatively narrow transects, then the layering structure of the forests (in this case forests near San Carlos on the Rio Negro, Venezuela) was displayed in the data. However, when wider transects were used to survey the same forest, the appearance of layers was lost from the data. *Chave et al.* [2004] found similar scale-related responses for the 50 ha mapped forest plot located in a moist tropical forest on Barro Colorado Island in Panama (Figure 1). They found the distribution of the aboveground biomass changes from a skewed and nonsymmetric form at small plots (0.04–0.1 ha), illustrating the gap dynamics to a symmetric and approximately normal form at large plots (0.5–1.0 ha), representing the equilibrium state. *Baker and Wilson* [2000] in developing a methodology of quantifying tree strata noted that transects wider than tree canopies confound the identification of forest strata. *Clark et al.* [2008] recently made direct collections of the leaf area height profiles of the tropical forest in La Selva, Costa Rica and found significant layering but could not resolve the horizontal extent of the layering phenomena (due to the nature of their sample design). They conjectured that it was likely to be the average horizontal extent of areas of similar forest height, approximately the size of the crowns of canopy trees. Similarly, *Parker and Brown* [2000] found that in temperate deciduous forests in Virginia, there is a strong dependency between the detection of strata and spatial resolution of samples. These observations have significant implications for the design of sampling density and scale for both ground and remote sensing measurements. Small plots (~0.1 ha) or resolutions (10–30 m) and large sampling density would be appropriate to capture the behavior of the forest gap dynamics, whereas large plots (~1.0 ha) or resolutions (~100 m) would be suitable to capture average behavior such as the forest biomass.

1.2.4. Biomass Estimators

[26] As discussed earlier, allometric equations are transfer functions to estimate the tree biomass from structural measurements (DBH, Height, Crown Size, etc.). These estima-

tors or equations have been developed using trees sampled from isolated sites or from small regions. Often, the equations are specific to individual species or group of species with growth characteristics of a region with specific climate, soil, and hydraulic conditions, hence extending such equations to other species or regions will introduce uncertainties in estimating the biomass. As a result, there are inherent errors in estimating forest biomass at large scales using the site specific estimators. These errors include (1) the use of coefficients derived for one species to another species, (2) sample trees and wood densities are not representative of target population because of size range and stand conditions, and (3) statistical errors in estimating coefficients or form of the estimators [*Jenkins et al.*, 2003]. Other factors such as inconsistent standards and methodologies in both sampling and development of equations, and measurements and data processing errors also impact the use of equations for large-scale forest biomass or carbon assessments. The propagation of errors from individual tree measurements to biomass equations depends on the spatial scale of the analysis. Errors in estimating the biomass density are potentially large at small scales (~0.1 ha) where the variability in structure and composition of forest are large and the forest is in nonequilibrium state, and small when the scale increases to 1.0 ha where the variability is small the forest structure approaches to an equilibrium and aggregate state [*Chave et al.*, 2004].

[27] Recently, several papers have reviewed allometric equations for trees in boreal forest and temperate forests [*Ter-Mikaelian and Korzukhin*, 1997; *Jenkins et al.*, 2003] as well as tropical forests [*Chave et al.*, 2005]. Jenkins et al. combine a large collection of allometric equations to develop generalized equations for large areas of North American forests. Chave et al. generalize over different tropical forests across the world. The relatively larger pool of sample sizes in these generalized equations tend to compensate for the lumping of trees across species and across the different physiognomic forms that trees of the same species can have in different settings. One also sees the general patterns that one would expect across collections of species: collected equations for angiosperms ("hardwoods") produce higher biomass values for a given diameter tree than gymnosperms ("softwoods"); the proportion of mass in branches for smaller angiosperms is higher than for comparable sized gymnosperms; foliage mass is higher in gymnosperms [*Jenkins et al.*, 2003]. One can use these results to produce aboveground biomass predictors. Information on the height of the trees (relating directly to capturing the variation in biomass associated with form) increases predictive capability for trees [*Chave et al.*, 2005].

2. Remote Sensing of Forest Structure

[28] Remote sensing, the process of imaging or sampling the interactions between electromagnetic energy and matter at selected wavelengths, has the ability to monitor terrestrial ecosystems at various temporal and spatial scales and has been widely tested for land cover mapping and various forestry applications [*Patenaude et al.*, 2005]. A remote sensing image of a landscape is composed of picture elements or pixels. Whether it is an aerial photograph, an airborne or spaceborne optical spectral image (AVIRIS, Landsat, MODIS), or an active microwave image generated with radar sensors, the spatial resolution of each pixel usually covers many trees. Viewing these images make several things readily apparent (Figure 5). Forests and woodlands appear quite different from cropland, range or peatlands, urban structures, water or bare soil. Within forested ecosystems other differences are apparent. Needleleaf canopies are quite distinct from broadleaf ones, and within each of these classes, young canopies can be readily distinguished from older ones. The reason for these differences is to a large extent dependent on the measurement approach (passive and active sensing) and the wavelength of observation (optical and microwave). However, optical properties of vegetation components, three-dimensional structure, tree architecture, and the spatial arrangement of leaves, branches, and stems are among the most important factors impacting the ability to distinguish vegetation communities using remote sensing. In addition to differences in the remote sensing observations among vegetation types, the spatial extent and horizontal variations in vegetation structure (tree density, canopy type, gap density, etc.) can be observed and monitored in the image data (Figure 6). As forest stands age, thinning in the stands and differences in the tree height and crown density distinguish one age class from another.

[29] In general, there are two types of remote sensing techniques: passive and active. There are a variety of subtle differences between these techniques. Passive sensing refers to sensors that detect or measure the reflected or emitted electromagnetic radiation from natural sources (radiation from the Sun in terms of visible and infrared photons, thermal, or microwave energy). Active sensing refers to sensors that detect reflected responses from objected irradiated from artificially generated energy sources, such as photons in lidar (light detection and ranging) and microwave energy in radar (radio detecting and ranging) sensors. Measurements from passive sensors are related to the hemispherically integrated reflection from the surface in all directions and hence are less sensitive to the vegetation structure, but more to optical properties (in visible and infrared wavelengths) and moisture (in thermal and microwave wavelength). However, several passive optical sensing techniques have been used to estimate vegetation canopy structure, horizontal variations from texture variations, or land cover extent and changes. Active sensors, on the other hand, measure reflection in one direction by penetrating into the vegetation canopies, and hence are more sensitive to the arrangement of objects (structure) on their propagation pathway. Radar and lidar sensors are currently being proposed as promising active techniques for a globally consistent and spatially resolved measurement of the vegetation three-dimensional structure and the above ground woody biomass from space and providing spatial data on vegetation structure, biomass and their changes due to disturbance and recovery processes.

2.1. Active Remote Sensing of Forest Structure

[30] Two active remote sensing sensors: imaging synthetic aperture radar (SAR), operating at large wavelengths (25–1 m) in fully polarimetric and interferometric (InSAR) modes, and multibeam lidar operating at 1064 nanometer wavelengths are the key sensors recommended for measurements of forest structure and biomass. These sensors measure

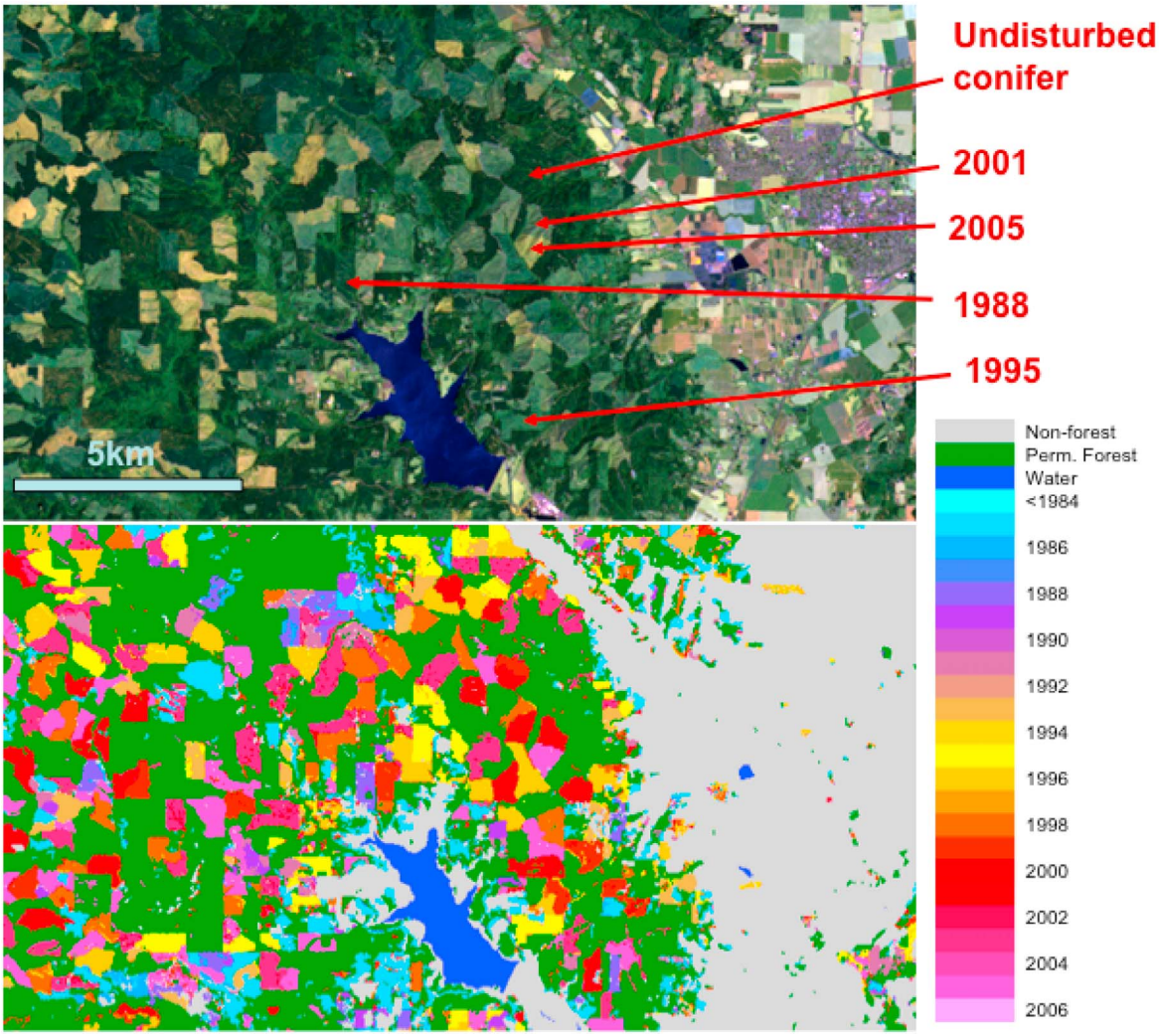

Figure 5. (top) Landsat-5 TM image (20 July 2005) from western Oregon (rgb equals 752 combinations) with arrows plus dates referring to the date of harvest; (bottom) date of disturbance (harvest) color coded, with permanent forest shown as dark green, nonforest shown as gray, and water shown as blue.

complementary characteristics of forest structure and biomass and their synergistic use from space can provide the most reliable data on the spatial distribution of the aboveground carbon stock and its changes.

2.1.1. Lidar Sensing of Structure

[31] Lidars emit nanosecond pulses of coherent light at the characteristic wavelength of its laser (a popular frequency is in the near infrared at 1064 nm). The pulses are emitted in the nadir or near-nadir direction and are scattered back into the lidar detectors by the land surface and its vegetated structures. The time elapsed since each pulse was fired and then received back at the instrument determines the distances to scattering events and the underlying terrain surface. The recorded signal or *lidar waveform* is a history of the laser return energy as a function of time. The shape of the waveform is a function of canopy height and vertical distribution of foliage, trunks, twigs, and branches at varying heights within the lidar footprint. The total waveform is therefore a measure of both the vertical distribution of vegetation surface area and the distribution of the underlying ground height [*Blair et al.*, 1999]. A lidar sensor also includes a processing and geolocation data system that evaluates each return waveform to extract relative timing points to allow the generation of topographic elevation and vertical structure parameters. The last pulse detected within the lidar waveform is the subcanopy ground response. The ground response is relatively easy to identify in more open (<90% canopy cover) forests and can be determined with accuracies on the order of centimeters.

[32] Differing lidar "metrics" related to canopy structure result from the manner in which the lidar waveform is processed [*Nilsson*, 1996; *Nelson*, 1997; *Means et al.*, 1999; *Lefsky et al.*, 1999; *Dubayah and Drake*, 2000; *Nelson et al.*, 2009a, 2009b]. Two different relative height (RH) metrics (relative to the ground return) are often used in estimating biomass within the lidar footprint: (1) RH100, the height relative to the ground over which 100 percent of the lidar energy from a pulse is returned, and (2) RH50, the height relative to the ground over with 50% of the lidar energy is returned. The lidar waveform also responds to the average vertical and horizontal stand structure. *Ni-Meister et al.* [2001] found that using the waveform to estimate the ver-

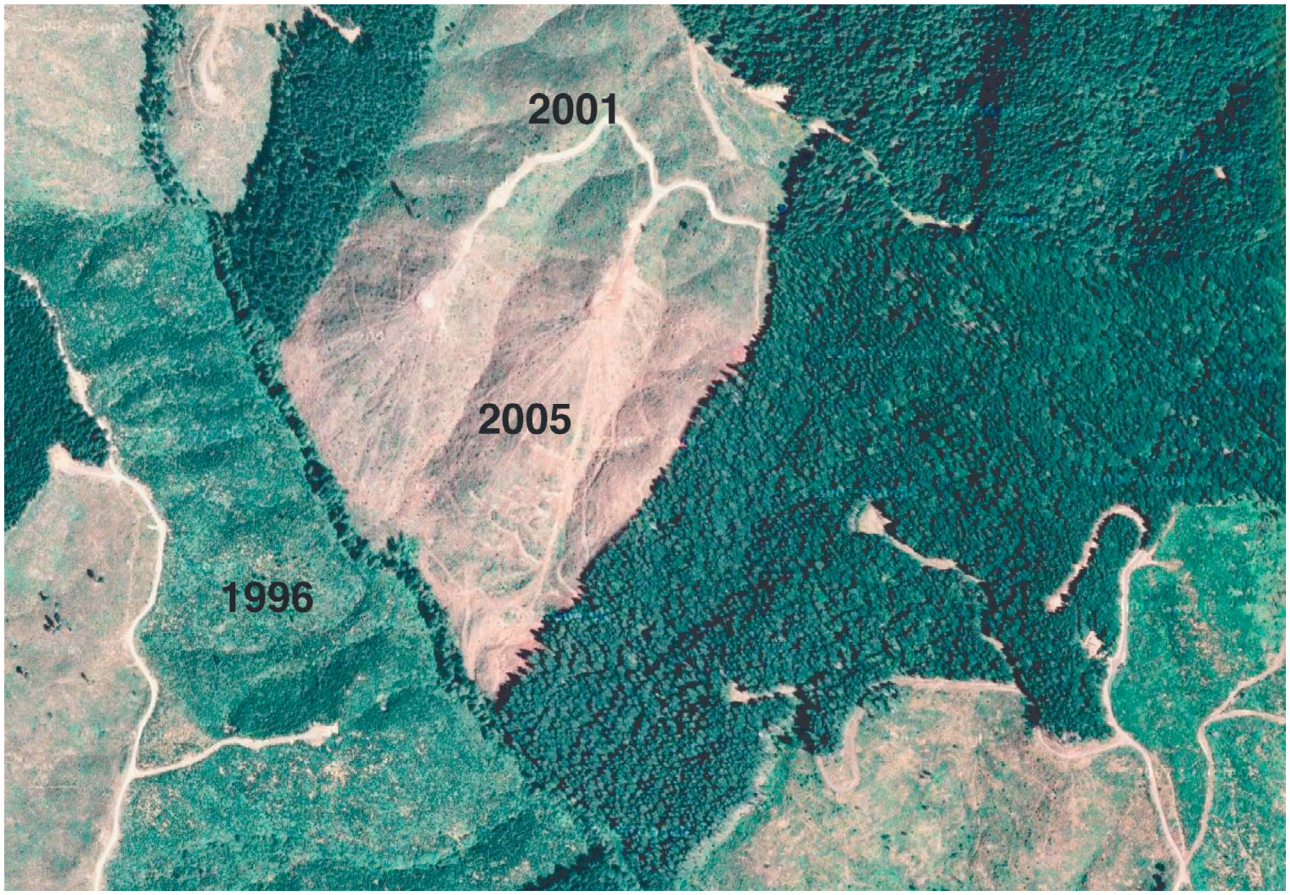

Figure 6. Google Earth true color close-up of a portion of Figure 5 area showing how patches of different age appear at higher resolution. (Google Earth imagery (c) Google Inc. Used with permission.)

tical profile of foliage area density for horizontally "clumped" canopies led to a significant error unless the horizontal heterogeneity was accounted for.

[33] Airborne lidar instruments can be designed to be either imaging or sampling. However, imaging lidar sensors for measuring vegetation structure have yet to fly in space. Only sampling lidar sensors are at a technology readiness level to be flown aboard orbiting platforms. The lidar profiles are rich in information related to vertical structure, and its distribution horizontally [*Drake et al.*, 2002a]. In addition to forest structure, forest biomass can be inferred from the height information contained in the vertical lidar profile [*Drake and Weishampel*, 2000; *Drake et al.*, 2002a, 2002b; *Lefsky et al.*, 2002; *Dubayah et al.*, 1997].

[34] A number of studies have shown that the difference between the first and last lidar returns and its various intermediate levels, measures of the height index of the forests in the lidar spot, are directly proportional to forest biomass, over a large range of ecosystem types [*Lefsky et al.*, 2005; *Drake et al.*, 2002b]. However, the accuracy of estimating forest height and biomass may vary depending on forest types [*Drake et al.*, 2002b; *Lefsky et al.*, 2005, 2007; *Anderson et al.*, 2006].

[35] Unfortunately, for now we are constrained to use only sampling lidars from space, but the sampled lidar information, when combined or fused with optical and radar imagery, promises a kind of "signature extension" of the lidar information from the points sampled, to entire images [*Ranson et al.*, 2007].

2.1.2. Radar Sensing of Structure and Biomass

[36] The imaging radar sweeps the landscape with the unique capability of its radio waves penetrating into the forest canopy and scattering from large woody components (stems and branches) that constitutes the bulk of biomass and carbon pool in forested ecosystems. The sensitivity of backscatter measurements at different wavelengths and polarizations to the size and orientation of woody components and their density makes the radar sensors suitable for direct measurements of live above ground woody biomass (carbon stock) and structural attributes such as volume and basal area. The recent innovations in orbital designs for repeat pass radar interferometry (InSAR) will also allow the sensor to measure the height of forests and provide a vertical dimension for accurately resolving the vegetation biomass over a variety of old growth and regenerating forests globally [*Balzter*, 2001]. Current state-of-the-art in radar technology allows *L* band (1.25 GHz) and *P* band (434 MHz) radar measurements from space with high spatial resolution (25–100 m), day and night imaging capability regardless of atmospheric conditions and cloud cover, and with a repeating global coverage at monthly to seasonal intervals. Such a system should be able to access information over forests globally, measure the magnitude of forest biomass in boreal and temperate regions, improve current estimates of forest

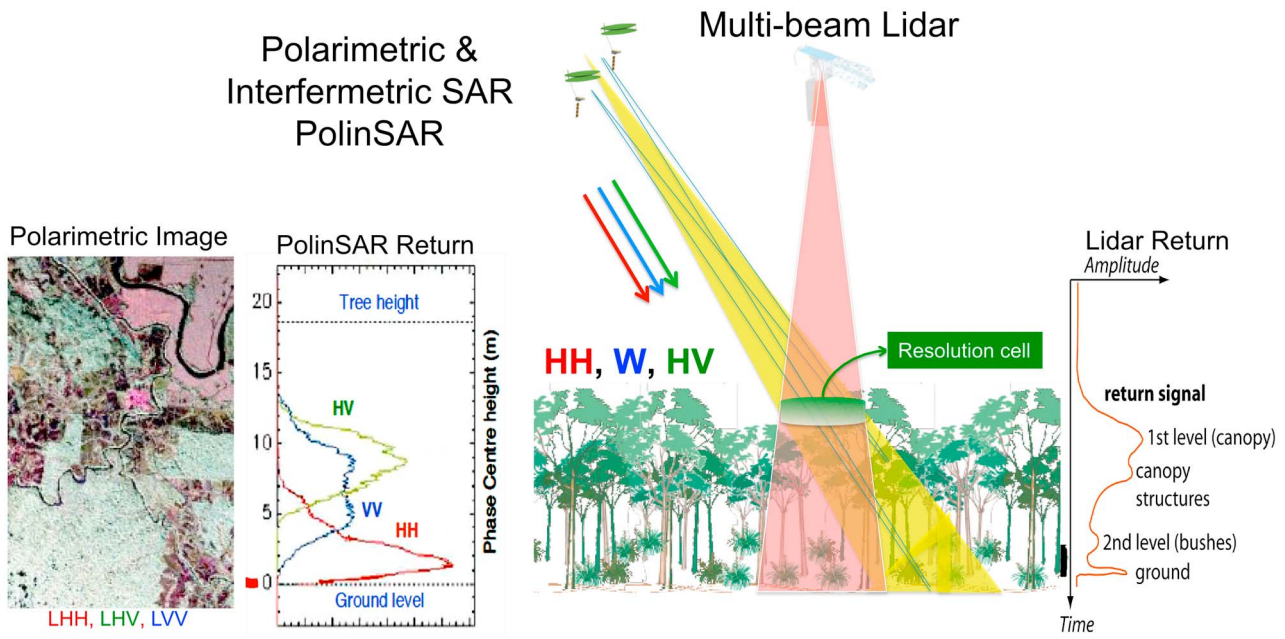

Figure 7. Radar imager maps of observed radar energy returned at various polarization transmit-receive combinations (HH, HV, VV, where H is horizontal polarization and V is vertical polarization) which are related to the volume and biomass of forest components. The multibeam lidar sampler measures the vertical variation in the strength of the scattered laser signal, which is related to forest vertical structure profile and biomass. The two signals are combined using "fusion" algorithms to improve the accuracy of radar estimates of biomass and to extend lidar measurements of structure in both space and time.

biomass in the tropics, monitor and identify changes of forest structure and biomass from disturbance (fire, logging, deforestation) and characterize post disturbance recovery.

[37] Radar measurements of forest structure and aboveground biomass can be divided into two approaches in the literature based on (1) polarimetric backscatter energy or (2) polarimetric InSAR (Pol-InSAR) measurements. In both cases, structure and biomass are estimated indirectly from radar measurements. In polarimetric backscatter measurements, forest components (stem, branch, and leaves) are scatterers within the footprint of the radar beam that interact with the incoming waves. The size (volume) and the dielectric constant (moisture or wood density) and orientation and morphology of the scatterers determine the magnitude and polarization of the reflected waves. As a result, the backscatter radar energy at linear polarizations (HH, HV, VV; H: Horizontal, and V: Vertical for transmit and receive configurations, respectively) is a function of the forest volume and biomass (Figure 7). The shape of this function is known to be dependent on wavelength, polarization, forest type and moisture conditions [*Dobson et al.*, 1992; *Le Toan et al.*, 1992]. In most studies, the cross-polarized (HV) term is shown to be most strongly correlated with the forest biomass. The estimation of biomass from backscatter measurements is exploited using either empirical statistical approaches or by inversion of physically based scattering models. In empirical statistical approaches, regression models are developed between the radar backscatter measurements at different frequencies or polarizations with forest structure (volume, basal area) and biomass components (stem and crown) obtained from field measurements [*Dobson et al.*, 1995; *Ranson et al.*, 1997; *Lucas et al.*, 2006; *Saatchi et al.*, 2007].

[38] Statistical approaches based on a single measurement may provide ambiguous estimates of biomass because of the impacts of other ecological and structural variables. By increasing the number of measurements (multiple polarizations, wavelength, and times) the estimation becomes less ambiguous [*Dobson et al.*, 1995; *Saatchi et al.*, 2007]. In model-based inversions, multiple measurements and simplifying assumptions are used to invert for key structural variables [*Saatchi and Moghaddam*, 2000]. In both cases, the errors associated with the biomass estimation can be reduced by increasing the wavelength of operation and by stratification of forest types based on structure and landscape types [*Dobson et al.*, 1995; *Saatchi et al.*, 2007].

[39] The loss of sensitivity to biomass with biomass increase produces a so-called saturation level, an upper bound on the range of biomass measured by radar backscatter power. This saturation is dependent on both radar wavelength, polarization mode, incidence angle as well as the type of forest, canopy structure and moisture conditions [*Ranson and Sun*, 1997]. As a result, there is a wide range of field-observed saturation levels depending on the conditions under which the radar measurements were acquired. In addition to saturation limit, the accuracy of biomass estimation plays a major role to define the limitations of radar sensors for biomass estimation [*Saatchi et al.*, 2010; *Le Toan et al.*, 2010]. In general, the loss of sensitivity introduces larger errors or an underestimation of biomass. The accuracy required for biomass estimation for a global measurement and monitoring system is less than 20% [*Houghton et al.*, 2009; *Frolking et al.*, 2009]. It is widely accepted that the *L* band backscatter power will provide biomass measurements of up to 100–150 Mg/ha with the above accuracy

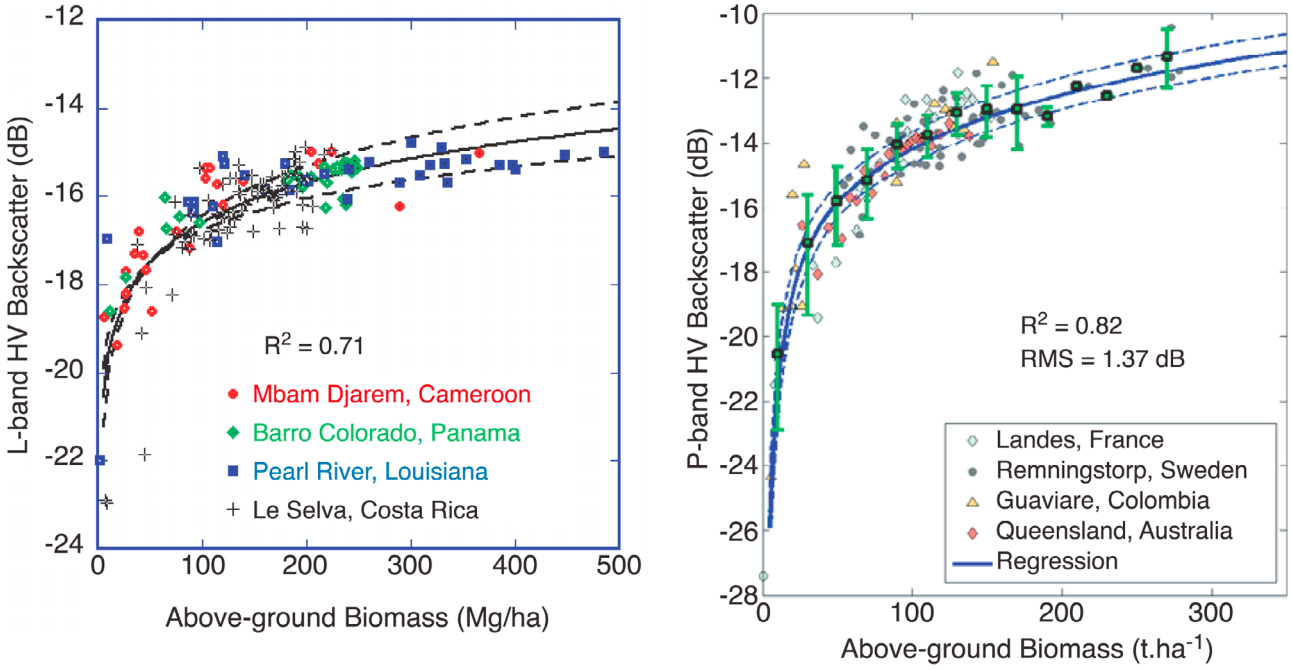

Figure 8. Relationship between backscatter power (in dB) at HV (horizontal transmit, vertical receive) polarization versus aboveground dry biomass (tons/ha). The best regression fit to the data is with logarithm of biomass. (left) Data extracted from ALOS PALSAR imagery over four study areas in tropical, temperate, and woodland savanna forests, (S. Saatchi, unpublished results, 2010). (right) Data extracted from *P* band airborne sensors from boreal, tropical, woodlands, and plantation forests [*Le Toan et al.*, 2010].

[*Kasischke et al.*, 1997]. However, at *L* band, reported saturation levels range from 60 Mgha^{-1} of biomass [*Luckman et al.*, 1998] in tropical forests using single polarization to about 200 Mgha^{-1} in boreal forests using multiple polarizations [*Ranson et al.*, 1995]. At *P* band this range may vary from 100 to 300 Mgha^{-1} in tropical forests [*Santos et al.*, 2003; *Hoekman and Quinones*, 2000; *Saatchi et al.*, 2010], and 200–300 Mgha^{-1} in boreal and temperate forests [*Rignot et al.*, 1994; *Dobson et al.*, 1995; *Kasischke et al.*, 1997; *Saatchi and Moghaddam*, 2000; *Saatchi et al.*, 2007]. Despite, the varying saturation range, radar backscatter with polarimetric measures and spatial textures have been used extensively to characterize or classify forests in terms of biomass and structure, even beyond the so-called saturation range [*Hoekman and Quinones*, 2000; *Saatchi and Moghaddam*, 2000; *Quinones and Hoekman*, 2004].

[40] In addition to measuring one-time biomass densities, imaging radar provides the capability of monitoring biomass changes resulting from forest disturbance [*Rowland et al.*, 2002; *Mitchard et al.*, 2010]. Acquiring multitemporal images at different polarizations and wavelengths allows detection of deforestation resulting from clear cutting, forest fires and insect disturbance, wind damage and to some extent changes in forest structure [*Saatchi and McDonald*, 1997; *Rignot et al.*, 1994; *Couturier et al.*, 2001; *Siegert et al.*, 2001; *Salas et al.*, 2002; *Ranson et al.*, 2003]. The results from these studies indicate the accuracy of monitoring forest disturbance and recovery by radar backscatter measurements and highlight various sources of errors and ambiguities. However, the results generally indicate that backscatter polarimetric measurements can potentially monitor disturbance modes in most global forested ecosystems (Figure 8).

[41] InSAR technique is based on the fact that radar backscatter contains information about the intensity and the phase of backscatter signal. The phase is determined by the two-way propagation length from the sensor to the resolution cell. By acquiring two complex SAR backscatter measurements over the same resolution cell from very close antenna positions (separated by a distance baseline), the phase difference associated with two viewing distances can be readily related to the three-dimensional position of the resolution cell [*Zebker et al.*, 1992]. Therefore, InSAR techniques were first used to measure surface topography such as in the SRTM (Shuttle Radar Topography Mission) [*Rodriguez et al.*, 2006] using either a single wavelength or single polarization sensors. Over vegetated surfaces, these observations showed a strong sensitivity to vegetation height and structure [*Rodriguez and Martin*, 1992; *Askne et al.*, 1997; *Treuhaft et al.*, 1996]. However, it was only recently that results from experiments and model developments showed that a combination of polarimetric and InSAR measurements can provide forest height and potentially three-dimensional structure over different forest types [*Papathanassiou and Cloude*, 2001; *Cloude*, 2007; *Balzter*, 2001; *Hajnsek et al.*, 2009].

[42] Although interferometry measurements are directly related to the height of the surface, over the vegetated surfaces, the InSAR coherence and phase are nonlinear functions of vegetation height, and as in backscatter case, the shape of the function depends wavelength, polarization, forest type, and canopy and surface moisture condition. Hence, the process of extracting vegetation height and structure, similar to backscatter case, involves either statistical regression or model inversion techniques [*Askne et al.*,

1997; *Cloude and Papathanassiou*, 1998]. Height estimation from Pol-InSAR, at large wavelengths (*L* band and *P* band), has been performed successfully over a variety of forest types [*Neumann et al.*, 2010; *Hajnsek et al.*, 2009; *Papathanassiou and Cloude*, 2001]. These results suggest that it is possible to derive an unambiguous derivation of height without a clear saturation level (*L* band and *P* band; Figure 8).

2.2. Passive Remote Sensing of Forest Structure Using Solar Radiation

[43] Passive remote sensing instruments measure vegetation properties indirectly by measuring the fraction of incident light that is reflected from the vegetation at different wavelengths. In forest stands, the sensors measure the aggregate reflectance as a function of wavelength (spectrum) of the tree canopies and understory within a pixel. The reflectance varies seasonally with phonological changes in the vegetation. The spectral reflectance spectrum is then exploited to extract information on forest structure, type, age, condition, biomass, leaf area, and even photosynthetic rate.

[44] The reflectance of a particular forest stand is determined by (1) the fraction of incident light that is scattered directly back into the sensor detectors from the canopy elements and the understory (sunlit canopy and understory) and (2) the fraction of light that is scattered multiple times from these elements, then into the sensor detectors (diffuse canopy and under story, or shadow). In the visible part of the spectrum the dominant signal detected by the sensor is the direct scattering, or sunlit canopy and sunlit under story. Multiple bounces of photons from the forest back to the sensor is small in comparison to direct scattering because the chlorophyll and other leaf pigments within the forest foliage are highly absorbing at visible wavelengths. At near infrared wavelengths, however, the foliage is more transparent and multiple scattering becomes more important. Hence, the near infrared wavelengths are sensitive to vegetation changes over a wider range of vegetation densities.

[45] In principle, given remote sensing measurements canopy reflectance at enough different wavelengths, the fraction of sunlit canopy and background and the fraction of shaded canopy and background can be inferred. These terms define the three-dimensional optical and morphological structure of the forest. The sunlit canopy reflectance is determined by the internal structure and optical properties of trees, the main factors being leaf reflectance and transmittance, related to leaf morphology and biochemistry, branch and bark reflectance, all characteristic of individual tree species, the leaf area, the leaf to branch area ratios, the leaf angle distribution etc. These factors give rise to very different reflectance for some species; for example some conifers and deciduous crowns have very different reflectance.

[46] Individual tree heights and shapes as well as stem density determine the shaded and sunlit fractions viewed by a sensor field of view. The 30 m resolution of Landsat and the 250 m and greater resolution of MODIS can include many individual trees of different morphologies, even nonforest cover types. Variations in these factors from one pixel to the next, introduce texture into the image, which can be used to extract further information related to the landscape-scale structures induced by the underlying topography, edaphic variations, and disturbance history. A number of studies have shown that the fraction of shadow in a pixel can in some cases be used to estimate stand biomass. For low-density canopies, the reflectance is exquisitely sensitive to spectral contrast between the sunlit canopy/background and the shadowed canopy/background. This contrast has been used very effectively to estimate biomass density [*Hall et al.*, 1995, 1996, 1997; *Peddle et al.*, 1999] by relating shadow and sunlit canopy fraction to canopy volume, hence biomass density.

3. Data Fusion

[47] Radar and lidar sensors provide complementary information about the forest structure from space. The volume of vegetation sensed by these two instruments at a pixel level is not exactly the same (Figure 7). However, the signatures have some level of commonality because of biophysical and structural nature of forest stands. The vertical distribution of reflective surfaces that can be inferred from lidar reveals the bole and branch structure supporting the leaves within a near vertical volume of the vegetation. Lidar sensors from space measure this vertical profile by sampling the forest stand along its orbital tracks. Radar provides imaging capability to estimate forest height through InSAR configuration or forest volume and biomass through polarimetric backscatter power. However, the vegetation signature from radar measurements is from a slanted volume and is sensitive to both vertical and horizontal arrangement of vegetation components (leaves, branches, and stems). The combination of the two sensors has the capability of providing the vegetation three-dimensional structure at spatial resolutions suitable for ecological studies (25–100 m). However, there are limited studies to explore the fusion of the two measurements because of the lack of data over the same study areas. Potentially, fusion between the two sensors can be exploited at three levels.

[48] 1. Parameter level, where forest structure such as height metrics, basal area and volume estimated by lidar and radar algorithms at a pixel level are combined in allometric equations to estimate stand-level forest biomass or other structural and biophysical parameters. This approach requires assessments of pixel-level structural parameters estimated from each sensor and careful consideration of spatial variability of forest structure at the stand level (spatial resolutions of greater than 100 m). The spatial averaging and comparison with stand-level ground measurements are important in this approach because lidar- and radar-estimated structures are not necessarily from the same vegetation volume or three-dimensional location. For example, leaves interact with the wavelengths of lidar emissions but are transparent to the wavelengths of *P* band radar. This differential sensitivity to targets of different dimensions represents a potential advantage for fusion because the sum of the range of structural element sizes detected by different sensors is greater than that of any one sensor alone.

[49] 2. Signal level, where radar backscatter or Pol-InSAR measurements are combined with lidar height metrics in statistical regression models to estimate forest three-dimensional structure (height, biomass, volume, basal area) [*Hyde et al.*, 2007; *Sun et al.*, 2008, 2002; *Slaton et al.*, 2001]. This approach is dependent on ground inventory data to

develop the statistical models and validate the results and hence requires careful assessment of the compatibility of inventory plot size and spatial resolution of remote sensing data.

[50] 3. Physical model level, where lidar measurements of vertical structure are used in radar backscatter and Pol-InSAR electromagnetic models to predict the radar returns and reduce the number of structural parameters in radar estimation algorithm. The advantage of this approach is that by including the physics of measurements and sensors' geometry, the uncertainty and errors due to variability in forest structure and sensor characteristics can be quantified. However, because of the large number of variables involved in developing a physically based model, in practice the fusion algorithms are developed for site-specific applications and will not be suitable for a globally operational system.

[51] 4. The fusion of active sensors with one another as well as the conjoining of active sensor information with information obtained from the existing constellation of passive remote sensing devices is currently limited by the lack of contemporaneous applications of the sensors at locations with well developed ground data. This will likely be an ongoing research area for several years to come.

4. Concluding Remarks

[52] Terrestrial ecosystem structure, seen as the three-dimensional arrangement of the vegetation at a location, determines the processing of water, essential elements and physical fluxes essential to understanding of the role of these ecosystems in the total Earth system. In forests, ecosystem structure is a statistical consequence of the sizes of trees, usually derived as a consequence of allometric transformations of statistical distributions of the diameters of trees. Remote sensing, particularly with active remote sensing, provides a capability to quantify the structure of forest systems by direct measurement of other indicators of structure. Theoretical, model-based investigations of the expected patterns of forest structure when measured at different scales indicates a fundamental difference in the fine-scale (approximately 0.10 ha) dynamics of forests and the larger-scale (approximately 10 ha) dynamics. The fine-scale dynamics of structure are cyclical, nonequilibrium kinetics associated with the birth, growth and death of a canopy dominant tree. In contrast, the large-scale dynamics are equilibrium seeking and a statistical-mechanical consequence of the fine-scale dynamics. What this implies for remote sensing of forest ecosystems structure is that a complete understand of the functioning of a forest requires measurement at both fine and large scales.

[53] **Acknowledgments.** This work was performed partially at the Jet Propulsion Laboratory, California Institute of Technology, under contract from National Aeronautic and Space Administration and the support of NASA's Terrestrial Ecology Program. We would also like to acknowledge the support to H. H. Shugart from NASA under grants NNX-07AF10G, NAG5-11084, NNX-07AO63G, NNX-08AL59G, NMO-710722, and NNG-05-GN69G.

References

Anderson, J., M. E. Martin, M.-L. Smith, R. O. Dubayah, M. A. Hofton, P. Hyde, B. E. Peterson, J. B. Blair, and R. G. Knox (2006), The use of waveform lidar to measure northern temperate mixed conifer and deciduous forest structure in New Hampshire, *Remote Sens. Environ.*, *105*, 248–261, doi:10.1016/j.rse.2006.07.001.

Askne, J. I. H., P. B. G. Dammert, L. M. H. Ulander, and G. Smith (1997), C-band repeat-pass interferometric SAR observations of the forest, *IEEE Trans. Geosci. Remote Sens.*, *35*, 25–35, doi:10.1109/36.551931.

Baker, P. J., and J. S. Wilson (2000), A quantitative technique for the identification of canopy stratification in tropical and temperate forests, *For. Ecol. Manage.*, *127*, 77–86, doi:10.1016/S0378-1127(99)00118-8.

Balzter, H. (2001), Forest mapping and monitoring with interferometric synthetic aperture radar (InSAR), *Prog. Phys. Geogr.*, *25*, 159–177.

Beauchamp, J. J., and J. S. Olson (1973), Corrections for bias in regression estimates after logarithmic transformation, *Ecology*, *54*, 1403–1407, doi:10.2307/1934208.

Blair, J. B., D. L. Rabine, and M. A. Hofton (1999), The Laser Vegetation Imaging Sensor: A medium-altitude, digitisation-only, airborne laser altimeter for mapping vegetation and topography, *ISPRS J. Photogramm. Remote Sens.*, *54*, 115–122, doi:10.1016/S0924-2716(99)00002-7.

Botkin, D. B., and L. Simpson (1990), Biomass of the North American Boreal Forest: A step toward accurate global measures, *Biogeochemistry*, *9*, 161–174.

Brown, S., A. J. R. Gillespie, and A. E. Lugo (1991), Biomass of tropical forests of South and Southeast Asia, *Can. J. For. Res.*, *21*, 111–117, doi:10.1139/x91-015.

Brunig, E. F., J. Heuveldop, and T. W. Schneider (1979), Dependence of productivity and stability on structure in natural and modified ecosystems in the tropical-rainforest-zone: Preliminary conclusions from the MAB pilot project at San Carlos de Rio Negro for the development of optimal agro-silvicultural and silvicultural systems, *Mitt. Bundesforschungsans. Forst Holzirtsch.*, *124*, 41–50.

Chambers, J. Q., J. dos Santos, R. J. Ribeiro, and N. Higuchi (2001), Tree damage, allometric relationships, and above-ground net primary production in a dense central Amazon forest, *For. Ecol. Manage.*, *152*, 73–84, doi:10.1016/S0378-1127(00)00591-0.

Chave, J., R. Condit, S. Lao, J. P. Caspersen, R. B. Foster, and S. P. Hubbell (2003), Spatial and temporal variation of biomass in a tropical forest: Results from a large census plot in Panama, *J. Ecol.*, *91*, 240–252, doi:10.1046/j.1365-2745.2003.00757.x.

Chave, J., R. Condit, S. Aguilar, A. Hernandez, S. Lao, and R. Perez (2004), Error propagation and scaling for tropical forest biomass, *Philos. Trans. R. Soc. London, Ser. B*, *359*, 409–420, doi:10.1098/rstb.2003.1425.

Chave, J., et al. (2005), Tree allometry and improved estimation of carbon stocks, *Oecologia*, *145*, 87–99, doi:10.1007/s00442-005-0100-x.

Clark, D. B., P. C. Olivas, S. F. Oberbauer, D. A. Clark, and M. G. Ryan (2008), First direct landscape-scale measurement of tropical rain forest Leaf Area Index: A key drive of global primary productivity, *Ecol. Lett.*, *11*, 163–172.

Cloude, S. R. (2007), Dual-baseline coherence tomography, *IEEE Geosci. Remote Sens. Lett.*, *4*, 127–131, doi:10.1109/LGRS.2006.885893.

Cloude, S. R., and K. P. Papathanassiou (1998), Polarimetric SAR interferometry, *IEEE Trans. Geosci. Remote Sens.*, *36*, 1551–1565, doi:10.1109/36.718859.

Couturier, S., D. Taylor, F. Siegert, A. Hoffmann, and M. Q. Bao (2001), ERS SAR backscatter: A potential real-time indicator of the proneness of modified rainforests to fire, *Remote Sens. Environ.*, *76*, 410–417, doi:10.1016/S0034-4257(01)00185-7.

Dobson, M. C., L. Pierce, K. Sarabandi, F. T. Ulaby, and T. Sharik (1992), Preliminary analysis of ERS-1 SAR for forest ecosystem studies, *IEEE Trans. Geosci. Remote Sens.*, *30*, 203–211.

Dobson, M. C., et al. (1995), Estimation of forest biophysical characteristics in northern Michigan with SIR-C/X-SAR, *IEEE Trans. Geosci. Remote Sens.*, *33*, 877–895, doi:10.1109/36.406674.

Drake, J. B., and J. F. Weishampel (2000), Multifractal analysis of canopy height measures in a longleaf pine savanna, *For. Ecol. Manage.*, *128*, 121–127, doi:10.1016/S0378-1127(99)00279-0.

Drake, J. B., R. O. Dubayah, D. B. Clark, R. G. Knox, J. B. Blair, M. A. Hofton, R. L. Chazdon, J. F. Weishampel, and S. Prince (2002a), Estimation of tropical forest structural characteristics using large-footprint lidar, *Remote Sens. Environ.*, *79*, 305–319, doi:10.1016/S0034-4257(01)00281-4.

Drake, J. B., R. O. Dubayah, R. G. Knox, D. B. Clark, and J. B. Blair (2002b), Sensitivity of large-footprint lidar to canopy structure and biomass in a neotropical rainforest, *Remote Sens. Environ.*, *81*, 378–392, doi:10.1016/S0034-4257(02)00013-5.

Dubayah, R. O., and J. B. Drake (2000), Lidar remote sensing for forestry, *J. For.*, *98*, 44–46.

Dubayah, R., J. B. Blair, J. Bufton, D. Clark, J. JáJá, R. Knox, S. Luthcke, S. Prince, and J. Weishampel (1997), The vegetation canopy lidar mission, in *Land Satellite Information in the Next Decade II: Sources and*

Applications, pp. 100–112, Am. Soc. for Photogramm. and Remote Sens., Bethesda, Md.

Fang, J., S. Brown, Y. Tang, G.-J. Nabuurs, X. Wang, and H. Shen (2006), Overestimated biomass carbon pools of the northern mid- and high-latitude forests, *Clim. Change*, *74*, 355–368, doi:10.1007/s10584-005-9028-8.

Frolking, S., M. W. Palace, D. B. Clark, J. Q. Chambers, H. H. Shugart, and G. C. Hurtt (2009), Forest disturbance and recovery: A general review in the context of spaceborne remote sensing of impacts on aboveground biomass and canopy structure, *J. Geophys. Res.*, *114*, G00E02, doi:10.1029/2008JG000911.

Fulton, M. R. (1999), Patterns in height-diameter relationships for selected tree species and sites in eastern Texas, *Can. J. For. Res.*, *29*, 1445–1448, doi:10.1139/cjfr-29-9-1445.

Greenhill, A. G. (1881), Determination of the greatest height consistent with stability that a vertical pole or mast can be made, and of the greatest height to which a tree of given proportions can grow, *Proc. Cambridge Philos. Soc.*, *4*, 65–73.

Hajnsek, I., F. Kugler, S.-K. Lee, and K. P. Papathanassiou (2009), Tropical-forest-parameter estimation by means of Pol-InSAR: The INDREX-II Campaign, *IEEE Trans. Geosci. Remote Sens.*, *47*, 481–493.

Hall, F. G., Y. E. Shimabukuro, and K. F. Huemmrich (1995), Remote sensing of forest biophysical structure in boreal stands of *Picea mariana* using mixture decomposition and geometric reflectance models, *Ecol. Appl.*, *5*, 993–1013, doi:10.2307/2269350.

Hall, F. G., D. R. Peddle, and E. F. LeDrew (1996), Remote sensing of biophysical variables in boreal forest stands of *Picea mariana*, *Int. J. Remote Sens.*, *17*, 3077–3081, doi:10.1080/01431169608949129.

Hall, F. G., D. E. Knapp, and K. F. Huemmrich (1997), Physically based classification and satellite mapping of biophysical characteristics in the southern boreal forest, *J. Geophys. Res.*, *102*(D24), 29,567–29,580.

Hallé, F., and R. A. A. Oldemann (1975), *Essay on the Architecture and Dynamics of Growth of Tropical Trees*, Penerbit Univ., Kuala Lumpur.

Hallé, F., R. A. A. Oldeman, and P. B. Tomlinson (1978), *Tropical Trees and Forests*, Springer, Heidelberg, Germany.

Hoekman, D. H., and M. J. Quinones (2000), Land cover and biomass classification using AirSAR data for evaluation of monitoring scenarios in the Colombian Amazon, *IEEE Trans. Geosci. Remote Sens.*, *38*, 685–696, doi:10.1109/36.841998.

Houghton, R. A., F. Hall, and S. J. Goetz (2009), Importance of biomass in the global carbon cycle, *J. Geophys. Res.*, *114*, G00E03, doi:10.1029/2009JG000935.

Hurtt, G. C., J. Fisk, R. Q. Thomas, R. Dubayah, P. R. Moorcroft, and H. H. Shugart (2010), Linking models and data on vegetation structure, *J. Geophys. Res.*, *115*, G00E10, doi:10.1029/2009JG000937.

Huston, M. A., and T. M. Smith (1987), Plant succession: Life history and competition, *Am. Nat.*, *130*, 168–198.

Hyde, P., R. Nelson, D. Kimes, and E. Levine (2007), Exploring lidar-radar synergy—Predicting aboveground biomass in a southwestern ponderosa pine forest using lidar, SAR and InSAR, *Remote Sens. Environ.*, *106*, 28–38, doi:10.1016/j.rse.2006.07.017.

Jansen, P. A., P. J. Van der Meer, and F. Bongers (2008), Spatial contagiousness of canopy disturbance in a tropical rain forest: An individual-tree-based test, *Ecology*, *89*, 3490–3502, doi:10.1890/07-1682.1.

Jenkins, J. C., D. C. Chojnacky, L. S. Heath, and R. A. Birdsey (2003), National-scale biomass estimators for United States tree species, *For. Sci.*, *49*, 12–35.

Jones, E. W. (1945), The structure and reproduction of the virgin forests of the north temperate zone, *New Phytol.*, *44*, 130–148, doi:10.1111/j.1469-8137.1945.tb05026.x.

Kasischke, E., J. Melack, and M. C. Dobson (1997), The use of imaging radars for ecological applications—A review, *Remote Sens. Environ.*, *59*, 141–156, doi:10.1016/S0034-4257(96)00148-4.

Kenderes, K., B. Mihók, and T. Standovár (2008), Thirty years of gap dynamics in a central European beech forest reserve, *Forestry*, *81*, 111–123, doi:10.1093/forestry/cpn001.

Kimmins, J. P. (1987), *Forest Ecology*, Macmillan, Vancouver, B. C., Canada.

Kira, T. (2001), *Forest and Environment: An Approach to Global Environmental Issues*, Shin-Shisosha, Tokyo.

Koch, G. W., S. C. Sillett, G. M. Jennings, and S. D. Davis (2004), The limits to tree height, *Nature*, *428*, 851–854, doi:10.1038/nature02417.

Köhl, M., C. T. Scott, and A. Zingg (1995), Evaluation of permanent sample surveys for growth and yield studies: A Swiss example, *For. Ecol. Manage.*, *71*, 187–194, doi:10.1016/0378-1127(94)06098-4.

Kuuluvainen, T. (1992), Tree architectures adapted to efficient light utilization: Is there a basis for latitudinal gradients?, *Oikos*, *65*, 275–284, doi:10.2307/3545019.

Landsberg, J. J., and R. H. Waring (1997), A generalised model of forest productivity using simplified concepts of radiation-use efficiency, carbon balance and partitioning, *For. Ecol. Manage.*, *95*, 209–228, doi:10.1016/S0378-1127(97)00026-1.

Lefsky, M. A., D. Harding, W. B. Cohen, G. Parker, and H. H. Shugart (1999), Surface lidar remote sensing of basal area and biomass in deciduous forests of eastern Maryland, USA, *Remote Sens. Environ.*, *67*, 83–98, doi:10.1016/S0034-4257(98)00071-6.

Lefsky, M. A., W. B. Cohen, D. J. Harding, G. G. Parker, S. A. Acker, and S. T. Gower (2002), Lidar remote sensing of above-ground biomass in three biomes, *Global Ecol. Biogeogr.*, *11*, 393–399, doi:10.1046/j.1466-822x.2002.00303.x.

Lefsky, M. A., D. J. Harding, M. Keller, W. B. Cohen, C. C. Carabajal, F. Del Bom Espirito-Santo, M. O. Hunter, and R. de Oliveira Jr. (2005), Estimates of forest canopy height and aboveground biomass using ICESat, *Geophys. Res. Lett.*, *32*, L22S02, doi:10.1029/2005GL023971.

Lefsky, M. A., M. Keller, Y. Pang, P. Camargo, and M. Hunter (2007), Revised method for forest canopy height estimation for Geoscience Laser Altimeter System waveforms, *J. Appl. Remote Sens.*, *1*, 013537, doi:10.1117/1.2795724.

Le Toan, T., A. Beaudoin, J. Riom, and D. Guyon (1992), Relating forest biomass to SAR data, *IEEE Trans. Geosci. Remote Sens.*, *30*, 403–411, doi:10.1109/36.134089.

Le Toan, T., S. Quegan, M. Davidson, H. Balzter, P. Paillou, K. Papathanassiou, S. Plummer, F. Rocca, S. Saatchi, and H. Shugart (2010), The BIOMASS mission: Mapping global forest biomass to better understand the terrestrial carbon cycle, *J. Remote Sens.*, in press.

Lucas, R. M., N. Cronin, A. Lee, M. Moghaddam, C. Witte, and P. Tickle (2006), Empirical relationships between AIRSAR backscatter and lidar-derived forest biomass, Queensland, Australia, *Remote Sens. Environ.*, *100*, 407–425, doi:10.1016/j.rse.2005.10.019.

Luckman, J., J. Baker, M. Honzak, and R. Lucas (1998), Tropical forest biomass density estimation using JERS-1 SAR: Seasonal variation, confidence limits and application to image mosaics, *Remote Sens. Environ.*, *63*, 126–139, doi:10.1016/S0034-4257(97)00133-8.

Manabe, T., K. Shimatani, S. Kawarasaki, S.-I. Aikawa, and S.-I. Yamamoto (2009), The patch mosaic of an old-growth warm-temperate forest: Patch level descriptions of 40 ear gap-forming processes and community structures, *Ecol. Res.*, *24*, 575–586, doi:10.1007/s11284-008-0528-7.

McDowell, N., et al. (2001), The relationship between tree height and leaf area:sapwood area ratio, *Oecologia*, *132*, 12–20.

McMahon, T. A. (1973), Size and shape in biology, *Science*, *179*, 1201–1204, doi:10.1126/science.179.4079.1201.

McMahon, T. A., and J. T. Bonner (1983), *On Size and Life*, Sci. Am. Libr., New York.

McMahon, T. A., and R. E. Kronauer (1976), Tree structures: Deducing the principle of mechanical design, *J. Theor. Biol.*, *59*, 443–466, doi:10.1016/0022-5193(76)90182-X.

Means, J. E., S. A. Acker, D. J. Harding, J. B. Blair, M. A. Lefsky, W. B. Cohen, M. E. Harmon, and W. A. McKee (1999), Use of large-footprint scanning airborne lidar to estimate forest stand characteristics in the Western Cascades of Oregon, *Remote Sens. Environ.*, *67*, 298–308, doi:10.1016/S0034-4257(98)00091-1.

Mitchard, E. T. A., S. S. Saatchi, I. H. Woodhouse, T. R. Feldpausch, L. S. Lewis, S. Sonké, and P. Meir (2010), Measuring biomass changes from woody encroachment and deforestation in the forest-savanna boundary region of central Africa from multi-temporal *L*-band radar backscatter, *Remote Sens. Environ.*, in press.

Nelson, R. (1997), Modeling forest canopy heights: The effects of canopy shape, *Remote Sens. Environ.*, *60*, 327–334, doi:10.1016/S0034-4257(96)00214-3.

Nelson, R., J. Boudreau, T. Gregoire, H. Margois, E. Naesset, T. Gobakken, and G. Stahle (2009a), Estimating Quebec provincial forest resources using ICESat/GLAS, *Can. J. For. Res.*, *39*, 862–881, doi:10.1139/X09-002.

Nelson, R., K. J. Ranson, G. Sun, D. S. Kimes, V. Kharuk, and P. Montesano (2009b), Estimating Siberian timber volume using MODIS and ICESat/GLAS, *Remote Sens. Environ.*, *113*, 691–701, doi:10.1016/j.rse.2008.11.010.

Neumann, M., L. Ferro-Famil, and A. Reigber (2010), Estimation of forest structure, ground, and canopy layer characteristics from multibaseline polarimetric interferometric SAR data, *IEEE Trans. Geosci. Remote Sens.*, *48*, 1088–1104.

Niklas, K. J. (1994), Interspecific allometries of critical buckling height and actual plant height, *Am. J. Bot.*, *81*, 1161–1168, doi:10.2307/2445478.

Niklas, K. J., and H.-C. Spatz (2004), Growth and hydraulic (not mechanical) constraints govern the scaling of tree height and mass, *Proc. Natl. Acad. Sci. U. S. A.*, *101*, 15,661–15,663, doi:10.1073/pnas.0405857101.

Nilsson, M. (1996), Estimation of tree heights and stand volume using an airborne lidar system, *Remote Sens. Environ.*, *56*, 1–7, doi:10.1016/0034-4257(95)00224-3.

Ni-Meister, W., D. L. B. Jupp, and R. Dubayah (2001), Modeling lidar waveforms in heterogeneous and discrete canopies, *IEEE Trans. Geosci. Remote Sens.*, *39*, 1943–1958, doi:10.1109/36.951085.

Papathanassiou, K. P., and S. R. Cloude (2001), Single-baseline polarimetric SAR interferometry, *IEEE Trans. Geosci. Remote Sens.*, *39*, 2352–2363, doi:10.1109/36.964971.

Parker, G. G., and M. J. Brown (2000), Forest canopy stratification—Is it useful?, *Am. Nat.*, *155*, 473–484, doi:10.1086/303340.

Patenaude, G., R. Milne, and T. P. Dawson (2005), Synthesis of remote sensing approaches for forest carbon sequestration: Reporting to the Kyoto protocol, *Environ. Sci. Policy*, *8*, 161–178, doi:10.1016/j.envsci.2004.12.010.

Peddle, D. R., F. G. Hall, and E. F. LeDrew (1999), Spectral mixture analysis and geometric optical reflectance modeling of boreal forest biophysical structure, *Remote Sens. Environ.*, *67*, 288–297, doi:10.1016/S0034-4257(98)00090-X.

Pretzsch, H. (2009), *Forest Dynamics, Yield and Growth: From Measurement to Model*, doi:10.1007/978-3-540-88307-4, Springer, Berlin.

Quinones, M. J., and D. H. Hoekman (2004), Exploration of factors limiting biomass estimation by polarimetric radar in tropical forests, *IEEE Trans. Geosci. Remote Sens.*, *42*, 86–104, doi:10.1109/TGRS.2003.815402.

Rackham, O. (1992), Mixtures, mosaics and clones: The distribution of trees within European woods and forests, in *The Ecology of Mixed-Species Stands of Trees*, edited by M. G. R. Cannell, D. C. Malcolm, and P. A. Robertson, pp. 1–20, Blackwell Sci., Oxford, U. K.

Ranson, K. J., and G. Sun (1997), An evaluation of AIRSAR and SIR-C/X-SAR images for mapping northern forest attributes in Maine, USA, *Remote Sens. Environ.*, *59*, 203–222, doi:10.1016/S0034-4257(96)00154-X.

Ranson, K. J., S. Saatchi, and G. Q. Sun (1995), Boreal forest ecosystem characterization with SIR-C/XSAR, *IEEE Trans. Geosci. Remote Sens.*, *33*, 867–876, doi:10.1109/36.406673.

Ranson, K. J., G. Sun, J. F. Weishampel, and R. G. Knox (1997), Forest biomass from combined ecosystem and radar backscatter modeling, *Remote Sens. Environ.*, *59*, 118–133, doi:10.1016/S0034-4257(96)00114-9.

Ranson, K. J., K. Kovacs, G. Sun, and V. I. Kharuk (2003), Disturbance recognition in the boreal forest using radar and Landsat-7, *Can. J. Remote Sens.*, *29*, 271–285.

Ranson, K. J., D. S. Kimes, G. Sun, V. Kharuk, and R. Nelson (2007), Using MODIS and GLAS data to develop timber volume estimates in central Siberia, in *International Geoscience and Remote Sensing Symposium, 2007*, pp. 2306–2309, doi:10.1109/IGARSS.2007.4423302, Inst. of Electr. and Electr. Eng., New York.

Richards, P. W. (1953), *The Tropical Rain Forest*, Cambridge Univ. Press, Cambridge, U. K.

Rignot, E., J. Way, C. Williams, and L. Viereck (1994), Radar estimates of above ground biomass in boreal forests of interior Alaska, *IEEE Trans. Geosci. Remote Sens.*, *32*, 1117–1124, doi:10.1109/36.312903.

Rodriguez, E., and J. M. Martin (1992), Theory and design of interferometric synthetic aperture radars, *IEE Proc. F Radar Signal Process.*, *139*, 147–159, doi:10.1049/ip-f-2.1992.0018.

Rodriguez, E., C. S. Morris, and J. E. Belz (2006), A global assessment of SRTM performance, *Photogramm. Eng. Remote Sens.*, *72*, 249–260.

Rowland, C., H. Balzter, T. Dawson, A. Luckman, L. Skinner, and G. Patenaude (2002), Biomass estimation of Thetford forest from SAR data: Potential and limitations, paper presented at ForestSAT, For. Res., For. Comm., Edinburgh, U. K., 5–9 Aug.

Ryan, M. G., and B. J. Yoder (1997), Hydraulic limits to tree height and growth, *BioScience*, *47*, 235–242, doi:10.2307/1313077.

Saatchi, S., and K. C. McDonald (1997), Coherent effects in microwave backscattering models for forest canopies, *IEEE Trans. Geosci. Remote Sens.*, *35*, 1032–1044.

Saatchi, S., and M. Moghaddam (2000), Estimation of crown and stem water content and biomass of boreal forest using polarimetric SAR imagery, *IEEE Trans. Geosci. Remote Sens.*, *38*, 697–709, doi:10.1109/36.841999.

Saatchi, S., K. Halligan, D. G. Despain, and R. L. Crabtree (2007), Estimation of forest fuel load from radar remote sensing, *IEEE Trans. Geosci. Remote Sens.*, *45*, 1726–1740, doi:10.1109/TGRS.2006.887002.

Saatchi, S., M. Marlier, R. Chazdon, D. Clark, and A. Russell (2010), Impacts of spatial variability of forest structure on radar estimation of aboveground biomass in tropical forests, *Remote Sens. Environ.*, in press.

Salas, W. A., M. J. Ducey, E. Rignot, and D. Skole (2002), Assessment of JERS-1 SAR for monitoring secondary vegetation in Amazonia: I. Spatial and temporal variability in backscatter across a chrono-sequence of secondary vegetation stands in Rondonia, *Int. J. Remote Sens.*, *23*, 1357–1379, doi:10.1080/01431160110092939.

Santos, J. R., C. C. Freitas, L. S. Araujo, L. V. Mura, F. F. Gama, L. S. Soler, and S. J. S. Sant'Anna (2003), Airbourne *P*-band SAR applied to the aboveground biomass studies in the Brazilian tropical rainforest, *Remote Sens. Environ.*, *87*, 482–493, doi:10.1016/j.rse.2002.12.001.

Shinozaki, K., K. Yoda, K. Hozumi, and T. Kira (1964), Quantitative analysis of plant form—The pipe model theory: I. Basic analysis, *Jap. J. Ecol.*, *14*, 97–105.

Shugart, H. H. (1990), Using ecosystem models to assess potential consequences of global climatic change, *Trends Ecol. Evol.*, *5*, 303–307, doi:10.1016/0169-5347(90)90086-S.

Shugart, H. H. (1998), *Terrestrial Ecosystems in Changing Environments*, 537 pp., Cambridge Univ. Press, Cambridge, U. K.

Shugart, H. H., and I. C. Prentice (1992), Individual tree-based models of forest dynamics and their application in global change research, in *A Systems Analysis of the Global Boreal Forest*, edited by H. H. Shugart, R. Leemans, and G. B. Bonan, pp. 313–333, doi:10.1017/CBO9780511565489.015, Cambridge Univ. Press, Cambridge, U. K.

Shugart, H. H., T. M. Smith, and W. M. Post (1992), The potential for application of individual-based simulation models for assessing the effects of global change, *Annu. Rev. Ecol. Syst.*, *23*, 15–38.

Shugart, H. H., W. R. Emanuel, and G. Shao (1996), Models of forest structure for conditions of climatic change, *Commonw. For. Rev.*, *75*, 51–64.

Shugart, H. H., L. L. Bourgeau-Chavez, and E. S. Kasischke (2000), Determination of stand properties in boreal and temperate forests using high-resolution photography and satellite imagery, *For. Sci.*, *46*, 478–486.

Siegert, F., G. Ruecker, A. Hinrichs, and A. A. Hoffmann (2001), Increased damage from fires in logged forests during droughts caused by El Niño, *Nature*, *414*, 437–440, doi:10.1038/35106547.

Slaton, M. R., E. R. Hunt Jr., and W. K. Smith (2001), Estimating near-infrared leaf reflectance from leaf structural characteristics, *Am. J. Bot.*, *88*, 278–284, doi:10.2307/2657019.

Smith, T. M., and D. L. Urban (1988), Scale and the resolution of forest structural pattern, *Vegetatio*, *74*, 143–150, doi:10.1007/BF00044739.

Sprugel, D. G. (1983), Correcting for bias in log-transformed allometric equations, *Ecology*, *64*, 209–210, doi:10.2307/1937343.

Sun, G., K. J. Ranson, and V. I. Kharuk (2002), Radiometric slope correction for forest biomass estimation from SAR data in the western Sayani Mountains, Siberia, *Remote Sens. Environ.*, *79*, 279–287.

Sun, G., K. J. Ranson, D. S. Kimes, J. B. Blair, and K. Kovacs (2008), Forest vertical structure from GLAS: An evaluation using LVIS and SRTM data, *Remote Sens. Environ.*, *112*, 107–117, doi:10.1016/j.rse.2006.09.036.

Swaine, M., and J. B. Hall (1988), The mosaic theory of forest regeneration and determination of forest composition in Ghana, *J. Trop. Ecol.*, *4*, 253–269, doi:10.1017/S0266467400002819.

Tadaki, Y., A. Sato, S. Sakurai, I. Takeuchi, and T. Kawahara (1977), Studies on the production structure of forest: XVIII. Structure and primary production in subalpine 'dead trees strips' *Abies* forest near Mt Asahi, *Jap. J. Ecol.*, *27*, 83–90.

Ter-Mikaelian, M. T., and M. D. Korzukhin (1997), Biomass equations for sixty-five North American tree species, *For. Ecol. Manage.*, *97*, 1–24, doi:10.1016/S0378-1127(97)00019-4.

Treuhaft, R. N., S. N. Madsen, M. Moghaddam, and J. J. van Zyl (1996), Vegetation characteristics and underlying topography from interferometric radar, *Radio Sci.*, *31*, 1449–1485, doi:10.1029/96RS01763.

Waring, R. H., and S. W. Running (1997), *Forest Ecosystems: Analysis at Multiple Scales*, Academic, San Diego, Calif.

Watt, A. S. (1947), Pattern and process in the plant community, *J. Ecol.*, *35*, 1–22, doi:10.2307/2256497.

Weishampel, J. F., D. L. Urban, H. H. Shugart, and J. B. Smith Jr. (1992), Semivariograms from a forest transect gap model compared with remotely sensed data, *J. Veg. Sci.*, *3*, 521–526, doi:10.2307/3235808.

Weishampel, J. F., G. Sun, K. J. Ranson, K. D. LeJeune, and H. H. Shugart (1994), Forest textural properties from simulated microwave backscatter: The influence of spatial resolution, *Remote Sens. Environ.*, *47*, 120–131, doi:10.1016/0034-4257(94)90149-X.

West, P. W. (2009), *Tree and Forest Measurement*, doi:10.1007/978-3-540-95966-3, Springer, New York.

West, G. B., and J. H. Brown (2005), The origin of allometric scaling laws in biology from genomes to ecosystems: Towards a quantitative unifying theory of biological structure and organization, *J. Exp. Biol.*, *208*, 1575–1592, doi:10.1242/jeb.01589.

West, G. B., J. H. Brown, and B. J. Enquist (1997), A general model for the origin of allometric scaling laws in biology, *Science*, *276*, 122–126, doi:10.1126/science.276.5309.122.

West, G. B., J. H. Brown, and B. J. Enquist (1999), A general model for the structure and allometry of plant vascular systems, *Nature*, *400*, 664–667, doi:10.1038/23251.

White, J. (1981), The allometric interpretation of the self-thinning rule, *J. Theor. Biol.*, *89*, 475–500, doi:10.1016/0022-5193(81)90363-5.

Whitmore, T. C. (1982), On pattern and process in forests, in *The Plant Community as a Working Mechanism*, *Spec. Publ. Br. Ecol. Soc.*, vol. 1, edited by E. I. Newman, pp. 45–59, Blackwell Sci., Oxford, U. K.

Williams, E. (2003), *Deforesting the Earth: From Prehistory to Global Crisis*, 689 pp., Univ. of Chicago Press, Chicago, Ill.

Zebker, H. A., S. N. Madsen, J. Martin, K. B. Wheeler, T. Miller, Y. Lou, G. Alberti, S. Vetrella, and A. Cucci (1992), The TOPSAR interferometric radar topographic mapping instrument, *IEEE Trans. Geosci. Remote Sens.*, *30*(5), 933–940, doi:10.1109/36.175328.

F. G. Hall, NASA Goddard Space Flight Center, Greenbelt, MD 20771, USA.

S. Saatchi, Jet Propulsion Laboratory, California Institute of Technology, Pasadena, CA 91109, USA.

H. H. Shugart, Department of Environmental Sciences, University of Virginia, Charlottesville, VA 22903, USA. (hhs@virginia.edu)